RSC Advances

ROYAL SOCIETY OF CHEMISTRY

www.rsc.org/advances

First-principles investigation of effects of Ni and Y co-doped on destabilized MgH_2

Gaili Sun,[a,b] Yuanyuan Li,[b] Xinxin Zhao,[a] Jianbao Wu,[a] Lili Wang*[a] and Yiming Mi*[a,b]

[a] College of Fundamental Studies, Shanghai University of Engineering Science, Shanghai 201620, China

[b] College of Chemistry and Chemical Engineering, Shanghai University of Engineering Science, Shanghai 201620, China

Abstract

The Ni and Y co-doping effect on structural stabilities and dehydrogenation properties of destabilized MgH_2 were studied by first-principles calculations. Ni and Y dopants prefer to occupy the Mg3 and Mg2 positions due to the minimal total electronic energy. The formation enthalpy was used to evaluated the stability of doped MgH_2 systems. Most of Ni and Y co-doped MgH_2 systems are more stable than Ni single-doping. Especially the case of x = 20 % ($Mg_8Ni_8Y_2H_{36}$) exhibits the highest stability. During the dehydrogenation process, the Ni and Y co-doped MgH_2 system possess promising dehydrogenation properties compare with pure Ni doping, which can be attributed to their relatively lower hydrogen desorption enthalpies. The electronic structures show that the hybridization of dopants with Mg and H atoms can strongly weaken Mg-H interactions, which effectively improve the dehydrogenation

*Corresponding authors.
E-mail addresses: llwang@sues.edu.cn (L.-L. Wang), yimingmi@sues.edu.cn (Y.-M. Mi).

properties of the Ni and Y co-doped MgH_2 system.

Keywords: First-principles calculation; Hydrogen storage; MgH_2; Stability; Enthalpy; Electronic structure.

1. Introduction

Metal hydrides with high hydrogen storage capacity and demonstrated cycling capability,[1-4] are considered to be some of the most promising hydrogen storage medium for the automotive applications. Among these hydrogen storage materials, magnesium hydride (MgH_2) has been investigated extensively in the last two decades as its high hydrogen storage capacity of 7.6 wt % and good reversibility,[5-7] together with the cheap cost and lightweight of magnesium.[8-9] Unfortunately, two technical obstacles limit the practical application of MgH_2: (i) high thermodynamic stability, which is responsible for the high dehydrogenation temperature requirement of 573 K at 1 bar H_2.[10-11] (ii) poor kinetics in the reaction of hydrogenation and dehydrogenation, which can be attributed to the low dissociation rate of H_2 on metallic Mg surface, a strong Mg-H bonding in magnesium hydride, and a slow hydrogen diffusion ability in MgH_2.[10-12]

To overcome these limitations in MgH_2, various efforts have been made to the design of Mg-based hydrogen storage materials. On one hand, reducing the gain size is an effective way to improve the thermodynamic behavior of MgH_2 by shortening the diffusion length, introducing defects and increasing the surface areas.[13-14] Theoretical calculations predicted that the reaction enthalpy of MgH_2 nanoparticles is reduced compared with the bulk material only when the particles are smaller than 2

nm containing < 50 Mg atoms.[15-16] However, this property is not straightforward for practical applications, because it is extremely difficult to prepare this size value of nanoparticles and keep the stabilities of these nanoparticles after repeated hydrogenation/dehydrogenation cycles.[17] On the other hand, introducing catalysts, such as transition metals, transition metals oxides, will improve hydrogen adsorption/desorption kinetics and thermodynamic properties of MgH_2. It is revealed that doping MgH_2 with transition metals can improve hydrogen adsorption/desorption kinetics as well as its thermodynamic properties. Many transition metals (TM), such as Ni, Ti, V, Zr, Fe, Ru, Co, Y, Rh, Pd, Cu, Ag and Nb, have been attempted as the documented additives for MgH_2.[18-24] Ren *et al*. found that V dopant can significantly reduce the dehydrogenation temperature and improve the kinetics of MgH_2.[20] Computational studies by Takahashi *et al*. used density functional theory (DFT) to investigate hydrogenation and dehydrogenation mechanism of Nb, NbO and Nb_2O_5 doped on MgH_2, and found that these dopants have a significant catalytic effect on dehydrogenation of MgH_2. [21-22] Dai *et al.* carried out first principles calculations based on DFT to show that Ni can improve the dehydrogenation properties of MgH_2 by weakened Mg-H bond.[23] Very recently, Hudson *et al.* discovered that graphene decorated Fe clusters dramatically improved the kinetics of MgH_2, and they provide the non-transition metal like graphene can be used as a catalyst for MgH_2 system.[24]

Previous studies[25-28] demonstrated that multiple transition metals additions are generally discovered to have a better effect in improving the hydrogenation performance of MgH_2 than does a single transition metals addition. It was found that

co-doped MgH_2 shows excellent hydrogen absorption/desorption kinetics, especially in the latter process, since it reduced the activation energies of both processes and weakened the Mg-H bonds. Zaluska *et al.* reported that the best storage kinetic results are contributed by a combination of the transition metals, such as V+Zr or Mn+Zr.[25] Another promising material is Mg-Ni-Y alloy, which can reach invertible hydrogen storage capacity of up to 5.3 wt% H_2. The rates of hydrogenation and dehydrogenation are up to 1 wt%-H/min at temperatures of 250℃, with remains nanocrystalline structure even after several cycles of H_2 uptake and release.[26] Li *et al.* investigated Mg alloyed 20 wt% Ni-Y and observed a high gravimetric hydrogen storage densities and excellent hydrogen sorption kinetics. At 293 K and 473 K under 3.0 MPa H_2, it can absorbed 4.16 and 5.59 wt% hydrogen, respectively. It can desorbed 4.75 wt% hydrogen in 15 min at 573 K under 0.1 MPa H_2.[27] Zhou *et al.* observed that Al and Y co-doped MgH_2 can weaken Mg-H bonds and promote hydrogen dissociate and desorption.[28] Moreover, the exact mechanism of Ni combined with Y as a catalyst in the enhancement of hydrogen storage properties of MgH_2 is not completely understood. Therefore, it is necessary to develop a systematic investigation of the synergistic effects of Ni with Y on improving the hydrogen storage properties of MgH_2.

In this paper, we performed a systematic study on the collaborative effects of Ni and Y co-doped with destabilized MgH_2 using first-principles calculations. The preferential sites of Ni and Y dopants on MgH_2 were determined by the lowest total electronic energy. The formation enthalpies and hydrogen desorption enthalpies were

used to study the dopants' influence on the structural stability and the dehydrogenation properties of the MgH_2. Electronic structures were analyzed to identify the intrinsic mechanisms of the dopants influence on bonding and dehydrogenation properties of the destabilized MgH_2 matrix.

2. Computational method

Energy and electronic structure calculations were performed under the framework of density functional theory (DFT) via Vienna Ab *initio* Simulation Package (VASP) code.[29-30] The projector augmented wave (PAW) method were used to span out the valence electron density, using the generalized gradient approximation (GGA) in the scheme of Perdew-Wang 91 (PW91) was adopted for the exchange-correlation functional.[31-32] For the plane wave basis set a cutoff energy of 350 eV was used throughout. The model of co-doped MgH_2 with Ni and Y were simulated by 3×3×1 and 3×3×3 supercells. The Brillouin-zone were sampled 3×3×7 and 3×3×3 Monkhorst-Pack k-point mesh for the supercells above, respectively. The electronic structures were defined self-consistent if the differences between two consecutive energies and forces be less than 10^{-7}eV and 0.01 eV/Å.

3. Results and discussion

3.1. Calculation models and site preference

MgH_2 has a tetragonal structure ($P4_2$/mnm, group No.136) with experimentally measured lattice parameters of a = 4.501 Å and c = 3.010 Å.[30] Two Mg atoms occupy the 2a (0, 0, 0) site and four H atoms occupy the 4f (0.303, 0.303, 0) site. In a previous work , we have calculated lattice parameters for a unit cell of MgH_2 are a =

4.477 Å and c = 2.989 Å, which are very close to the experimental[34] and other theoretical results.[35-36] The model of MgH_2 were built from 3×3×1 supercell and computed using those bulk parameters. The 3×3×1 supercell (see Fig. 1.) contained a total of 54 atoms with four non-equivalent position for Mg and six non-equivalent position for H. The optimal atomic positions of Mg and H atoms are good agreement with theoretical data.[28]

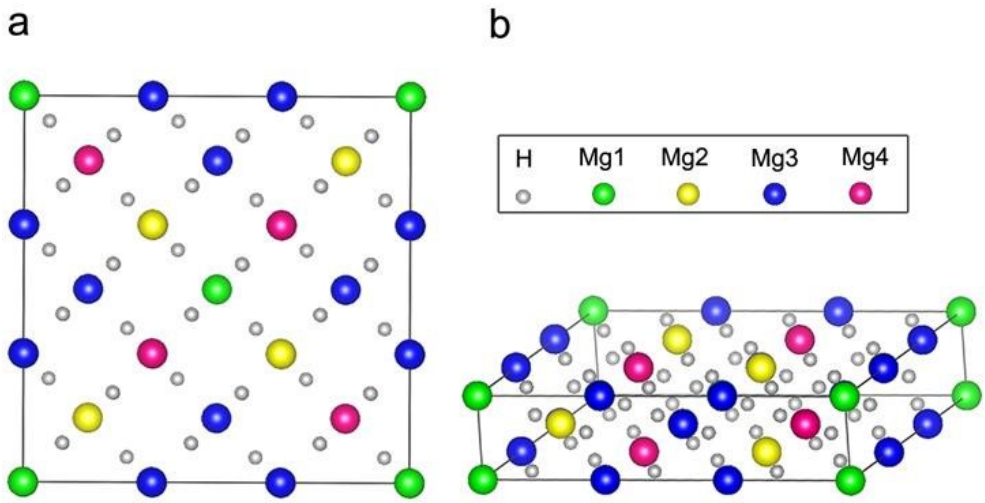

Fig. 1 Top (a) and side (b) views of MgH_2 3×3×1 supercell model. Mg1, Mg2, Mg3 and Mg4 denote four non-equivalent position for Mg, respectively.

In order to find the optimum geometry and doped sites of dopants (Ni and Y) in MgH_2, each of the four non-equivalent positions of Mg is substituted by Ni in order. The calculated total electronic energies of Ni doping system are shown in Fig. 2(a). These results suggest that Ni atom prefers to stayed in the Mg3 position, due to the minimal total electronic energy. And the new compounds are denoted as (Mg, Ni)H_2. Then, Mg is substituted by Y in the other three non-equivalent positions (Mg1, Mg2 and Mg4) of (Mg, Ni)H_2 compound. The calculated total electronic energies are shown in Fig.2(b). Y atom is likely to substitutes for the Mg2 position due to its

lowest total electronic energy. The new compounds are denoted as (Mg, Ni, Y)H_2. Adoping the same method, we also calculate total electronic energies of different doped site of dopants (Ni and Y) in MgH_2 3×3×3 supercell. The calculated total electronic energies of these doping systems are shown in Fig.2(c) and Fig.2(d). Ni and Y are prefer to occupy Mg3 and Mg2 positions in 3×3×3 supercell, respectively. The calculated results of 3×3×3 supercell are consistent with the results of 3×3×1 supercell, we have chosen the latter results in the following calculations due to 3×3×1 supercell model has a higher calculation efficiency.

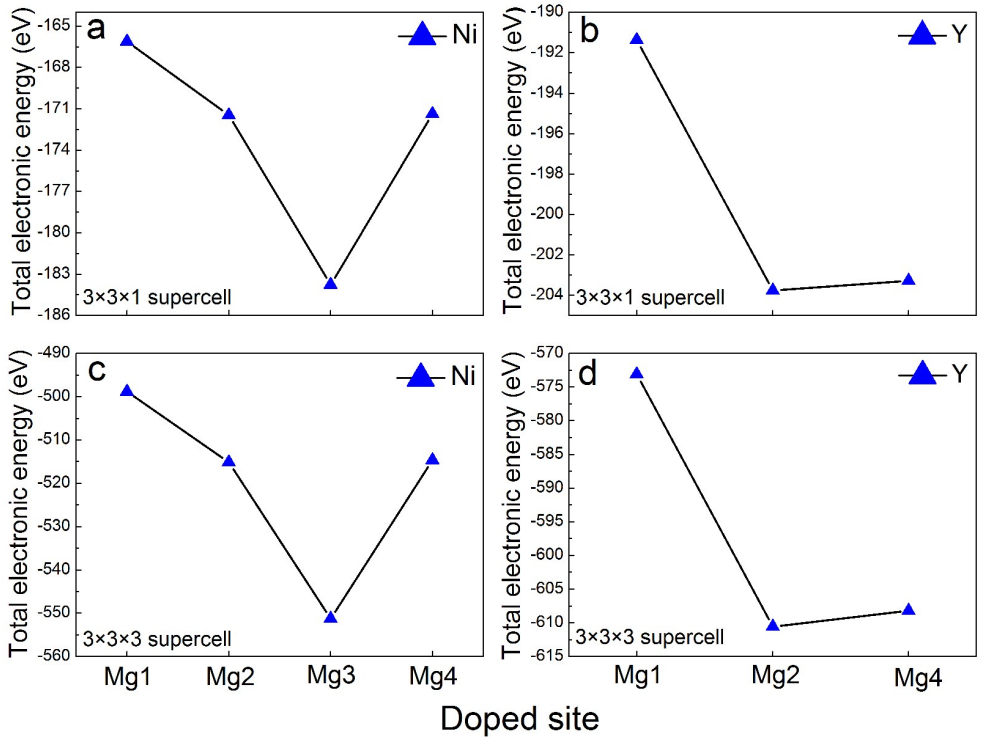

Fig.2 The total electronic energy for: (a) doping MgH_2 (3×3×1 supercell) with Ni in four non-equivalent positions of Mg; (b) doping (Mg, Ni)H_2 (3×3×1 supercell) with Y in the other non-equivalent positions of Mg; (c) doping MgH_2 (3×3×3 supercell) with Ni in four non-equivalent positions of Mg; (d) doping (Mg, Ni)H_2 (3×3×3 supercell) with Y in the other non-equivalent positions of Mg;

In order to systematic investigation the role of Ni and Y co-doping on structural stability of MgH_2, we studied the substitution of Mg2 by Y in different doping concentrations. Therefore, we chose eight doping concentrations of x = 0, 10 %, 13 %, 20 %, 27 %, 30 %, 33 % or 40 % in (Mg, Ni)H_2, which means substituting n = 0, 1, 1.3, 2, 2.7, 3, 3.3 or 4 out of 10 Mg atoms in $Mg_{10-n}Ni_8Y_nH_{36}$. For the case of 1.3, 2.7 or 3.3 out of 10 Mg atoms in $Mg_{10-n}Ni_8Y_nH_{36}$, we perform an equivalent treatment by replacing 4, 8 or 10 of 30 Mg atoms in (Mg, Ni)H_2 (3×3×3) supercell to achieve the doping level of x = 13 %, 27 % or 33 % in (Mg, Ni)H_2. The chosen method of preferential positions in different concentrations keeps consistent with that used in former.

The favorability of single-doping and co-doping in MgH_2 can be identified by the substitution energies (E_{sub}), which were calculated via the following definition:[38-39]

$$E_{sub} = 1/54[E_t(Mg_{10-n}Ni_8M_nH_{36}) - E_t(Mg_{18}H_{36}) - 8E_b(Ni) - nE_b(Y) + (8 + n)E_b(Mg)] \quad (1)$$

where E_t(M) refers to the total energies of hydrides in supercells. E_b represents the total energies per atom in the bulk structure. The obtained substitution energies of the doped materials with different Y concentrations are presented in Fig. 3. It can be seen that Ni and Y co-doped MgH_2 systems have lower substitution energy value compare with Ni single doped system, except the doping concentrations of x = 10 % ($Mg_9Ni_8YH_{36}$) and 33 % ($Mg_{6.8}Ni_8Y_{3.3}H_{36}$). Compared with Ni single-doped system,

the substitution energy of $Mg_9Ni_8YH_{36}$ and $Mg_{6.8}Ni_8Y_{3.3}H_{36}$ are increased slightly by about 2.6 % and 2.9 %, respectively. Furthermore, the lowest substitution energy value is located at the doping concentrations of x = 20 % ($Mg_8Ni_8Y_2H_{36}$), which is lowered that of Ni single-doping by 65.9 %. From energy point of view, the smaller substitution energy corresponds to the more favorable substitution doping. Hence, most of the co-doping Ni and Y into MgH_2 is more energetically favorable than the single-doping. In particular, the case of x = 20 % ($Mg_8Ni_8Y_2H_{36}$) is the most energetically favorable doping.

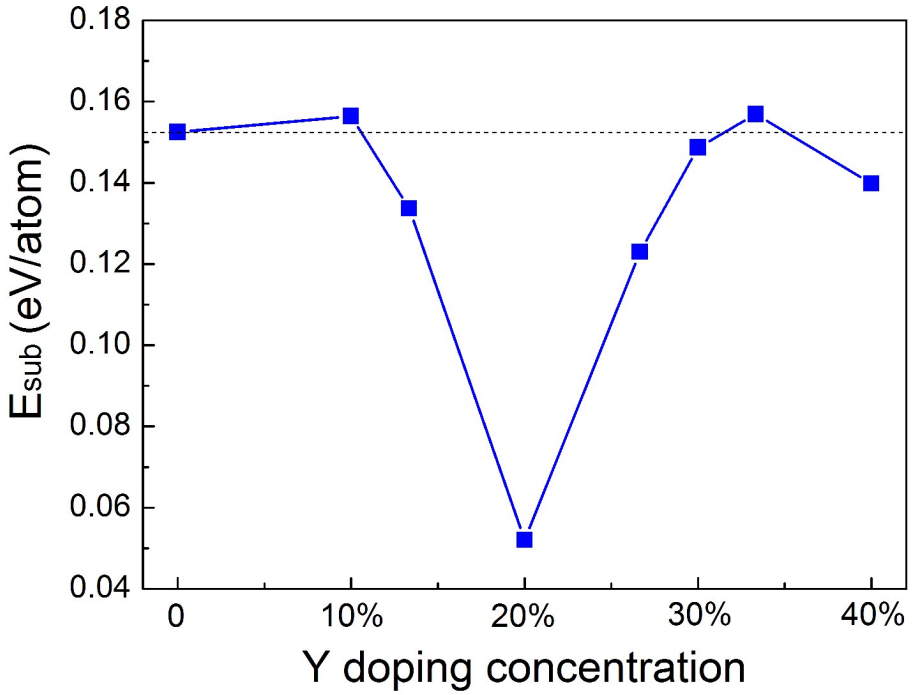

Fig.3 The calculated substitutional energies (E_{sub}) of the doped hydrides with different Y concentrations of x = 0, 10 %, 13 %, 20 %, 27 %, 30 %, 33 % or 40 %.

3.2. Stability and dehydrogenation properties

Commonly, the structural stability of crystal can be evaluated by its formation enthalpy ΔH_{form}. A negative formation enthalpy indicates that the crystal can exist

stably. Besides, a lower formation enthalpy suggests a stronger stability.[40] In order to investigate the stability of Ni and Y doping on MgH_2 system, the formation enthalpies ΔH_{form} are calculated by using equation (2):[28,40-41]

$$\Delta H_{form} = 1/54[E_t(Mg_{10-n}Ni_8Y_nH_{36}) - 8E_s(Ni) - nE_b(Y) - (10 - n)E_b(Mg) - 18E(H_2)] \quad (2)$$

where E_t(M) refers to the total energies of hydrides in supercells. E_b represents the total energies per atom in the bulk structure. The total energy of free H_2 molecule, $E(H_2)$, was computed as -6.77 eV using a 8 $Å^3$ cubic cell, consistent with other theoretical results.[28,47] The calculated formation enthalpy of the doped hydrides with different Y concentrations are presented in Fig. 4. The formation enthalpies of these eight compounds are found to be all negative, which indicates they can exist stably. Otherwise, Ni and Y co-doped MgH_2 systems have lower formation enthalpy value compare with Ni single-doped system, except the doping concentrations of x = 10 % ($Mg_9Ni_8YH_{36}$) and 33 % ($Mg_{6.8}Ni_8Y_{3.3}H_{36}$). Compared with Ni single-doped system, the formation enthalpy of $Mg_9Ni_8YH_{36}$ and $Mg_{6.8}Ni_8Y_{3.3}H_{36}$ are increased by about 6.5 % and 17.8 %, respectively. Furthermore, the case of x = 20 % ($Mg_8Ni_8Y_2H_{36}$) has the lowest enthalpy value, which is lowered that of Ni single-doping by 172.6 %. The trend is consistent with the calculated results of the substitution energy. Hence, the doping Ni combined with Y into MgH_2 exhibits higher stability than Ni single-doping. Especially the doping concentration of x = 20 % ($Mg_8Ni_8Y_2H_{36}$) exhibits the highest stability.

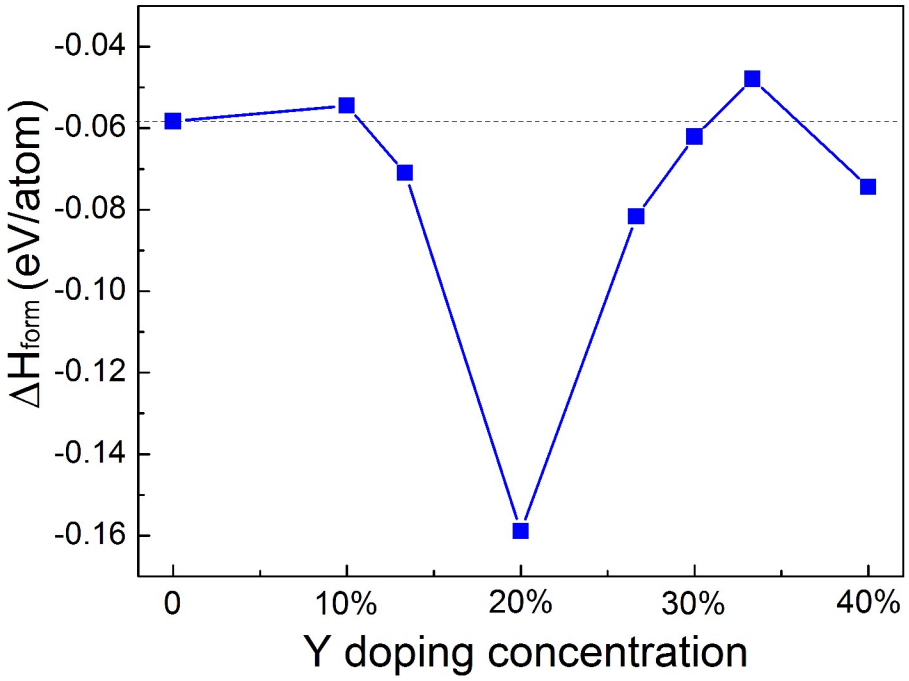

Fig.4 The calculated formation enthalpies (ΔH_{form}) of the doped hydrides with different Y concentrations of x = 0, 10 %, 13 %, 20 %, 27 %, 30 %, 33 % or 40 %.

From the investigation of the substitution energy and the formation enthalpy above, $Mg_8Ni_8Y_2H_{36}$ is more energetically favorable than other co-doping compounds. Therefore, about the dehydrogenation property, bond and electronic structure of the Ni and Y co-doped system, we are going to investigating the case of the Y doping concentration of x = 20 % ($Mg_8Ni_8Y_2H_{36}$) for co-doped systems, comparing to Ni single-doping case.

In order to further assess the dehydrogenation abilities of these hydrides, their hydrogen desorption enthalpies ΔH_{des} are calculated by using equation(3):[42-43]

$$\Delta H_{des} = [E_t(Mg_{10-n}Ni_8Y_nH_{35}) + 1/2E(H_2)] - E_t(Mg_{10-n}Ni_8Y_nH_{36}) \quad (3)$$

where $E_t(Mg_{18-n}Ni_8Y_nH_{36})$ represents the total energy of hydrides. $E_t(Mg_{10-n}Ni_8Y_nH_{35})$ refers to a pseudostructure in which one H atoms are removed from the relaxed $E_t(Mg_{18-n}Ni_8Y_nH_{36})$ system. $E(H_2)$ is the same as that used in equations (2).

The obtained hydrogen desorption enthalpy (ΔH_{des}) in single-doped MgH_2 with Ni is 0.71 eV. This enthalpy value is lower than the result in Ref.[10], which may be ascribed to the higher dopant content here. Moreover, compared with the value of ΔH_{des} = 1.5335 eV result for pure MgH_2,[44-45] the hydrogen desorption enthalpy of single-doped MgH_2 system is decreased. After Ni doping, the lower hydrogen desorption enthalpy of doped MgH_2 system leads to a improvement of its dehydrogenation properties. For the best Ni and Y co-doped MgH_2 system, the hydrogen desorption enthalpies by moving out one H atom from each of six non-equivalent positions of the co-doped system are all calculated. The obtained hydrogen desorption enthalpies (ΔH_{des}) are presented in Fig. 5. It can be observed that the hydrogen desorption enthalpies of this hydride are all singnificantly decreased in comparison with the Ni single-doped and pure MgH_2 systems. Thus every hydrogen desorption is much easier than single-doped case, which indicates the Ni and Y co-doping system exhibits excellent dehydrogenation properties. Besides, parts of these hydrogen desorption enthalpies of Ni and Y co-doped MgH_2 system are lower than that of alloying MgH_2 with other catalysts.[21,24,28] Based on the calculated results, we can conclude that co-doped MgH_2 with Ni and Y not only enhanced the structural stability of MgH_2, but also is beneficial to the improvement of dehydrogenation properties for MgH_2. Although the partial substitution of Mg by Ni and Y has significant synergetic effects on MgH_2, the detailed understanding of the influence of dopants about the hydrogen desorption process and kinetics of MgH_2 requires a further investigated, which will be the subject of our future work.

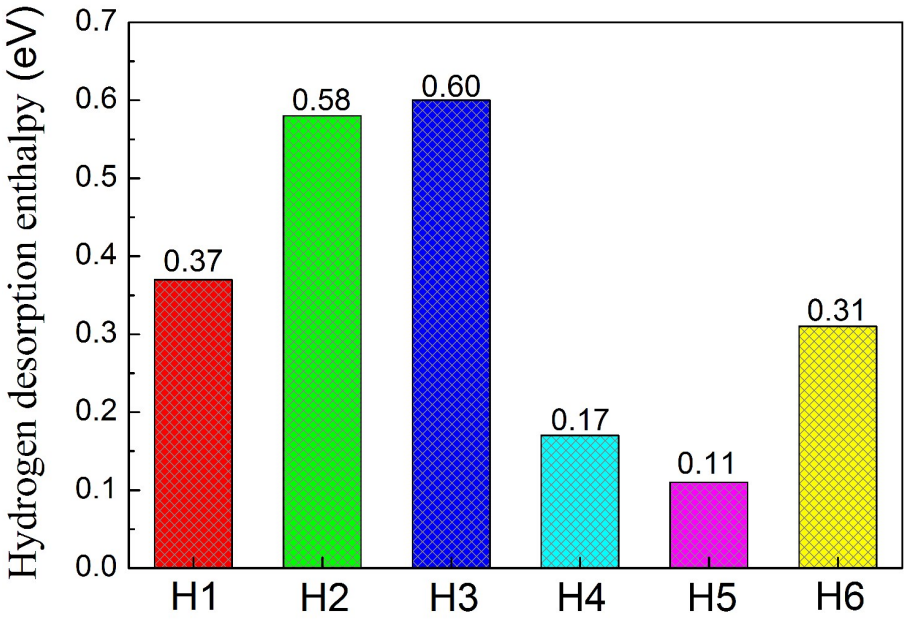

Fig.5 The calculated hydrogen desorption enthalpies (ΔH_{des}) by moving out one H atom (H1-H6) for Y the doping concentrations of x = 20 % ($Mg_8Ni_8Y_2H_{36}$) in (Mg, Ni)H_2.

3.3. Bonding analysis

Table 1 lists the bond distances between metallic elements in undoped and doped MgH_2. For undoped MgH_2, the bond length of Mg-Mg range from 3.50 Å to 4.48 Å with an average length of 3.66 Å. For Ni single-doped MgH_2 system, Mg2, Mg4 are the nearest neighboring metallic atom of the dopant Ni and the Mg-Ni bonds are decreased by an average of 3.90 Å. Discounting radius difference, the bond length of Mg-Ni is longer than the original Mg-Mg, which implies the Mg-Ni bond is weakened. But the bond length of Mg-Mg is decreased, thus the strength of Mg-Mg bond is enhanced compared with the pure MgH_2. For the best co-doped case of $Mg_8Ni_8Y_2H_{36}$, discounting radius difference, the distances between the Mg and Ni atoms are decreased in comparison with that of the single-doped system, indicates that its bond strength are strengthened. Furthermore, the length of Mg-Y bond and the Y-Ni bond are shorter than the Ni-doped system, thus the bond strength of Mg-Y and Y-Ni are

enhanced. These can be inferred that the dopant Y has strong alloying trend with Mg and Ni atoms, which would be weakened the strength of Mg-H and Ni-H bonds.

Table 1 Calculated the bond distance (Å) between metallic elements in the hydrides

MgH_2	Mg1-Mg2	Mg1-Mg3	Mg1-Mg4	Mg2-Mg3	Mg2-Mg4	Mg3-Mg4
	3.50	4.48	3.50	3.50	3.50	3.50
$Mg_{10}Ni_8H_{36}$	Mg1-Mg2	Mg1-Ni	Mg1-Mg4	Mg2-Ni	Mg2-Mg4	Ni-Mg4
	3.28	4.34	3.28	3.46	3.21	3.31
$Mg_8Ni_8Y_2H_{36}$	Mg1-Mg2	Mg1-Ni	Mg1-Mg4	Mg2-Ni	Mg2-Mg4	Ni-Mg4
	3.87	3.81	3.25	3.07	3.13	3.04
	Mg1-Y			Y-Ni	Y-Mg4	
	3.36			3.09	3.40	

Table 2 lists the interaction of metallic and H atoms in undoped and doped MgH_2. In this calculation, the bond length of Mg-H ranges from 1.93 Å to 1.94Å with an average of 1.93 Å, consistent with the experimental[34] and other theoretical results.[35-36] For Ni single-doped MgH_2 system, H4, H5 and H6 atoms are the nearest neighboring atoms of dopant Ni and these atoms move towards Ni, thus the bond length of Mg-H (H4-H6) are increased. Meanwhile, the Mg-H (H5, H6) bond length is also increased. Hence, the bond strength of Mg-H is weakened. For Ni and Y co-doped MgH_2 ($Mg_8Ni_8Y_2H_{36}$), the nearest neighboring H (H4-H5) atoms of Ni further move towards the Ni, thus the Mg-H (H4-H5) bonds further weaken their strength. But the Ni-H6 bond is a little bit weaken. H1, H3 and H6 atoms are the nearest neighboring atoms of the dopant Y, comparison with single-doped system, the bond length of Y-H (H1-H6) is markedly increased. The length of Mg-H bond are all increased, Which means the strength of Mg-H bond are all weakened. Therefore, the dopant Y can further weaken the Mg-H bond.

Table 2 Calculated the bond distance (Å) between metallic and H atoms in the hydrides								
$Mg_{10}Ni_8H_{36}$	Mg1-H1	1.80	Mg2-H1	1.84	Ni-H4-1	1.78	Mg4-H2	1.79
	Mg1-H2	1.84	Mg2-H3	1.80	Ni-H4-2	1.62	Mg4-H3	1.77
			Mg2-H6	2.25	Ni-H5	1.66	Mg4-H5	1.95
					Ni-H6	1.68		
$Mg_8Ni_8Y_2H_{36}$	Mg1-H1	1.83	Mg2-H1	3.46	Ni-H4-1	1.72	Mg4-H2	2.00
	Mg1-H2	1.91	Mg2-H3	1.88	Ni-H4-2	1.62	Mg4-H3	1.83
			Mg2-H6	2.30	Ni-H5	1.59	Mg4-H5	1.99
			Y-H1	2.16	Ni-H6	1.70		
			Y-H3	2.11				
			Y-H6	2.45				

3.4. Electronic structure

Fig. 6(a) shows the total and partial density of states (DOS) of undoped MgH_2. the Fermi energy (E_F) level is set at zero. The gap between the valence band (VB) and conduction band (CB) is about 4 eV, in good agreement with other calculation results.[28,46] The relatively large gap value of bulk leads to a relatively high formation energy. The VB is mainly dominated by H s states and the CB mainly by Mg s and Mg p states. Analyzing the partial DOS curves, these correspond to the strong ionic bonding interactions between Mg and H atoms. By using the Bader charge analysis in molecule AIM theory[47-49], it is found that the average electron number of Mg and H atoms is 0.42 and 1.79, respectively, as shown in Table 3. The ionic charges of Mg and H can be represented as $Mg^{1.58+}$ and $H^{0.79-}$, indicating the strong ionic character of Mg-H bond.

Table 3 Bader charges for undoped and doped MgH_2 systems

MgH_2	Mg1	Mg2	Mg3	Mg4		
	0.43	0.42	0.42	0.42		
	H1	H2	H3	H4	H5	H6
	1.79	1.79	1.79	1.80	1.79	1.79
$Mg_{10}Ni_8H_{36}$	Mg1	Mg2	Ni	Mg4		
	0.44	0.41	9.63	0.43		
	H1	H2	H3	H4	H5	H6
	1.79	1.78	1.81	1.22	1.61	1.32
$Mg_8Ni_8Y_2H_{36}$	Mg1	Mg2	Y	Ni	Mg4	
	0.44	0.39	9.33	9.66	0.43	
	H1	H2	H3	H4	H5	H6
	1.76	1.79	1.75	1.23	1.62	1.33

Fig. 6(b) shows the total and partial DOS of Ni single-doped MgH_2 system. In order to plot the partial DOS of all atoms in the same panel with the same scale, the amplitude of the partial DOS of Ni d orbital was decreased by 10. The total DOS curve shows a remarkable decrease in the band gap of 0 eV, which show clearly metallic characteristics. It can be obviously seen that Ni d states insert in the middle part and then overlapped with Mg p and H s orbitals separately in a different energy region. The electrons in Mg p and H s hybridization states are pushed to Mg p, Ni d and H s hybridization states. The interactions of Mg-H bond in these regions are weakened. Furthermore, the H s orbitals distributed in the region of -5.5 to -3.1 eV are less overlapped with Mg s and p orbitals comparing to pure MgH_2, which can help to weaken the hybridization of Mg-H bond. This interpretation is also supported by the Bader charge data. As shown in Table 3, the bader charges on H (H4-H6) atoms decrease significantly and the bader charges on Mg (Mg1, Mg4) increase slightly after Ni-doping. Therefore, the electron transfer from H to Mg is obviously weakened.

Fig. 6(c) shows the total and partial DOS of the Ni and Y co-doped MgH_2 system, this case corresponds to a Y doping concentration of x = 20 % ($Mg_8Ni_8Y_2H_{36}$). In

order to plot the partial DOS of all atoms in the same panel with the same scale, the amplitude of the partial DOS of Ni d and Y d orbitals were decreased by 10 and 5, respectively. The main peaks of co-doped system slightly move away from the Fermi energy compared with Ni single-doped MgH_2, implying a higher stability of Ni and Y co-doped system. The Y p and d orbitals overlap with H s, Mg p, Ni p and d orbitals in the energy region of -6.0 to -2.6 eV. And the distributions of bonding peaks of Y d orbitals are mainly concentrated in the energy region of 1.2 to 5.1 eV and overlap well with Mg s and p orbitals. These behaviors indicate that Y atom has strong bonding interaction with H, Mg and Ni atoms and decreases Mg-H p-s mixing. In addition, the drop of magnitude of bonding peaks of H s, Mg s and p orbitals are more than that of Ni single-doping, which means that Mg-H bond is further weakened in co-doped system. Similar the Ni single-doped system, this interpretation is also supported by the Bader charge data. The number of electrons around H (H1, H3) atoms in co-doped system is decreased compared with Ni single-doped MgH_2, which imply that the the electron transfer from H to Mg is further weakened. Thus, the Mg-H hybridizations are significantly weakened by Ni and Y co-doping.

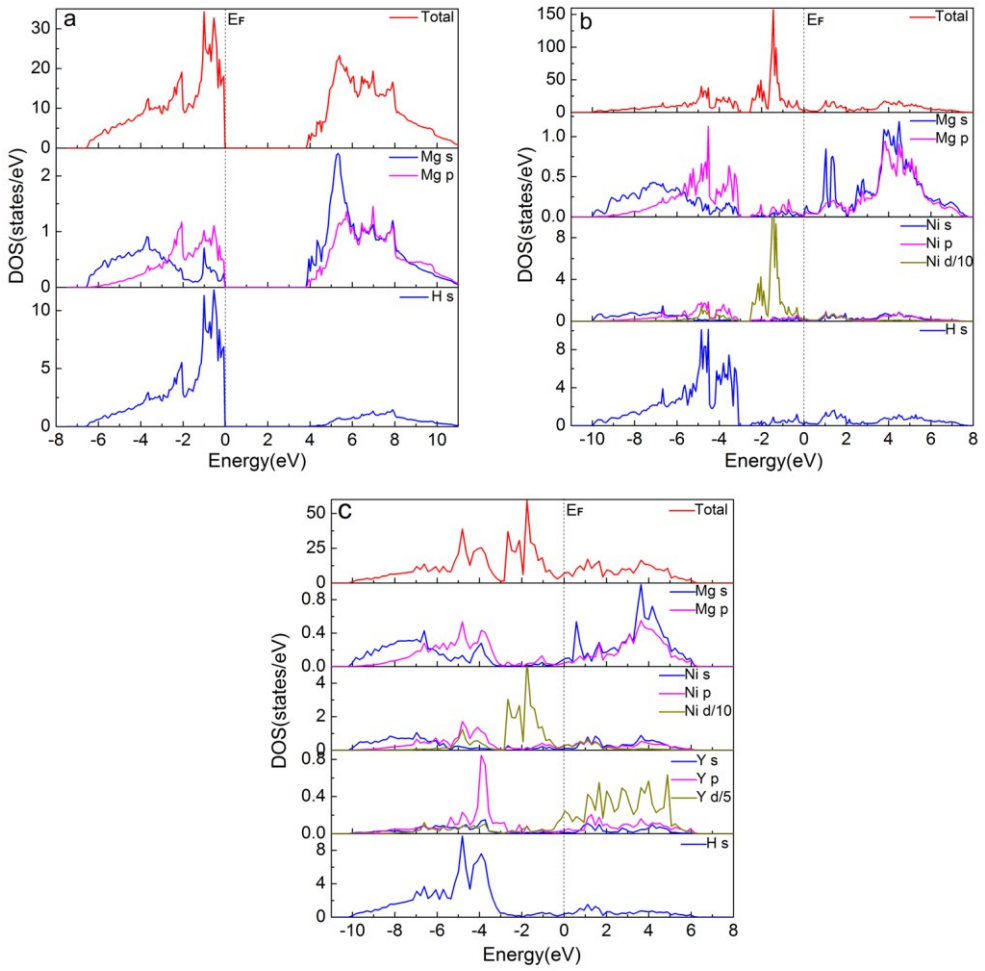

Fig.6 Total and partial densities of states (DOS) of (a) undoped MgH_2; (b) $Mg_{10}Ni_8H_{36}$; (c) $Mg_8Ni_8Y_2H_{36}$.

4. Conclusion

In summary, first-principles calculations were preformed to study the structural stabilities and dehydrogenation properties of destabilized MgH_2 co-doped with Ni and Y. According to the minimal total electronic energy, the Ni and Y prefer to substitute the Mg3 and Mg2 position, respectively. The substitution energies and formation enthalpies of different Y doping concentrations of hydrides were estimated. It shows that most of Ni and Y co-doped MgH_2 systems are more stable than Ni single-doping. Especially, the Y doping concentrations of x = 20% ($Mg_8Ni_8Y_2H_{36}$) has most energetic

stability. Moreover, this calculations also give insight into the hydrogen desorption enthalpies (ΔH_{des}) of this cases. The Ni and Y co-doped MgH_2 systems has the lowest ΔH_{des} value of 0.11 eV. Due to the relatively lower hydrogen desorption enthalpy, Ni and Y co-doped MgH_2 system possess promising dehydrogenation properties. The electronic structures show that the hybridization of dopants with Mg and H atom together weaken the Mg-H interaction. The electronic structures further demonstrates that Mg-H bonds are more susceptible to dissociate by Ni and Y co-doping because of the reduced magnitude of Mg-H hybridization peaks. Therefore, the co-doping with Ni and Y effectively improve the dehydrogenation properties of destabilized MgH_2.

Acknowledgments

The work was supported by the National Natural Science Fund (No.11504228) and the Graduated Innovative Research Project of Shanghai University of Engineering Science (No.E1-0903-14-01107-14KY0411).

REFERENCES

1 S. Q. Hao and D. S. Sholl, *J. Phys. Chem. C*, 2012, **116**, 2045-2050.

2 J. J. Tang, X. B. Yang, L. J. Chen and Y. J. Zhao, *AIP Adv.*, 2014, **4**, 077101.

3 J. H. Dai, Y. Song and R. Yang, *J. Phys. Chem. C*, 2010, **114**, 11328-11334.

4 Y. Zhong, H. Zhu, L. L. Shaw and R. Ramprasad, *J. Phys. Chem. C*, 2010, **114**, 21801-21807.

5 D. Meggiolaro, G. Gigli, A. Paolone, F. Vitucci and S. Brutti, *J. Phys. Chem. C*, 2013, **117**, 22467-22477.

6 M. Ismail, N. Juahir and N. S. Mustafa, *J. Phys. Chem. C*, 2014, **118**, 18878-

18883.

7 S. Q. Hao and D. S. Sholl, *J. Phys. Chem. Lett.*, 2010, **1**, 2968-2973.

8 T. Jiang, L. X. Sun and W. X. Li, *Phys. Rev. B*, 2010, **81**, 035416.

9 Q. Wan, P. Li, J. W. Shan, F. Q. Zhai, Z. L. Li and X. H. Qu, *J. Phys. Chem. C*, 2015, **119**, 2925-2934.

10 J. H. Dai, Y. Song and R. Yang, *J. Phys. Chem. C*, 2010, **114**, 11328-11334.

11 J. Zhang, D. W. Zhou, P. Peng and J. S. Liu, *Physica B*, 2008, **403**, 4217-4223.

12 J. J. Tang, X. B. Yang, M. Chen, M. Zhu and Y. J. Zhao, *J. Phys. Chem. C*, 2012, **116**, 14943-14949.

13 M. Chen, X. B. Yang, J. Cui, J. J. Tang, L. Y. Gan, M. Zhou and Y. J. Zhao, *Int. J. Hydrogen Energy*, 2012, **37**, 309-317.

14 J. J. Liu, J. Tyrrell, L. Cheng and Q. F. Ge, *J. Phys. Chem. C*, 2013, **117**, 8099-8104.

15 R. W. Wagemans, J. H. van Lenthe, P. E. de Jongh, A. Josvan Dillen and K. P. de Jong, *J. Am. Chem. Soc.*, 2005, **127**, 16675-16680.

16 K. C. Kim, B. Dai, J. K. Johnson and D. S. Sholl, *Nanotechnology*, 2009, **20**, 204001.

17 S. Cheung, W. Q. Deng, A. C. T. van Duin and W. A. Goddard, *J. Phys. Chem. A*, 2005, **109**, 851-859.

18 H. C. Wang, D. H. Wu, L. T. Wei and B. Y. Tang, *J. Phys. Chem. C*, 2014, **118**, 13607-13616.

19 M. Pozzo and D. Alfè, *Int. J. Hydrogen Energy*, 2009, **34**, 1992-1930.

20 C. Ren, Z. Z. Fang, C. S. Zhou, J. Lu, Y. Ren and X. Y. Zhang, *J. Phys. Chem. C*, 2014, **118**, 21778-21784.

21 K. Takahashi, S. Isobe and S. Ohnuki, *J. Alloy Compd.*, 2013, **58**, S25-S28.

22 K. Takahashi, S. Isobe and S. Ohnuki, *Langmuir*, 2013, **29**, 12059-12065.

23 Y. Mina, H. W. Hanno and Z. Y. Zhang, *Phys. Rev. B*, 2011, **83**, 045413.

24 M. S. L. Hudson, K. Takahashi, A. Ramesh, S. Awasthi, A. K. Ghosh, P. Ravindran and O. N. Srivastava, *Catal. Sci. Technol.*, 2015, **6**, 261-268.

25 A. Zaluska, L. Zaluski and J. O. Strom-Olsen, *J. Alloy Compd.*, 1999, **288**, 217-215.

26 S. Kalinichenkaa, L. Röntzschb and B. Kiebacka, *Int. J. Hydrogen Energy*, 2009, **34**, 7749-7755.

27 Z. N. Li, X. P. Liu, L. J. Jiang and S. M. Wang, *Int. J. Hydrogen Energy*, 2007, **32**,1869-1874.

28 S. C. Zhou, R. K. Pan, T. P. Luo, D. H. Wu, L. T. Wei and B. Y. Tang, *Int. J. Hydrogen Energy*, 2014, **39**, 9254-9261.

29 G. Kresse and J. Hafner, *Phys. Rev. B*, 1993, **47**, 558-561.

30 G. Kresse and J. Furthmüler, *Phys. Rev. B*, 1996, **54**, 11169-11187.

31 P. E. Blöchl, *Phys. Rev. B*, 1994, **50**, 17953-17979.

32 J. P. Perdew and Y. Wang, *Phys. Rev. B*, 1992, **45**, 13244-13249.

33 E. Callini, L. Pasquini, T. R. Jensen and E. Bonetti, *Int. J. Hydrogen Energy*, 2013, **38**, 12207-12212.

34 S. Ono, Y. Ishido, K. Imanari, T. Tabata, Y. Cho, R. Yamamoto and J. Less.

Common Met., 1982, **88**, 57-61.

35 Y. Bouhadda, A. Rabehi and S. Bezzari-Tahar-Chaouche, *Rev. Energies Renouvelables*, 2007, 10, 545-550.

36 M. Bortz, B. Bertheville, G. Böttger and K. Yvon, *J. Alloy Compd.*, 1999, **287**, L4-6.

37 L. W. Huang, O. Elkedim, M. Nowak, R. Chassagnon and M. Jurczyk, *Int. J. Hydrogen Energy*, 2012, **37**, 14248-14256.

38 Y. Song, W. C. Zhang and R. Yang, *Int. J. Hydrogen Energy*, 2009, **34**, 1389-1398.

39 Y. Song, Z. X. Guo and R. Yang, *Phys. Rev. B*, 2004, **69**, 094205.

40 T. Fischer and J. Almlof, *J. Phys .Chem.*, 1992, **96**, 9768-9774.

41 B. Y. Tang, N. Wang, W. Y. Yu, X. Q. Zeng and W. J. Ding, *Acta Mater*, 2008, **279**, 192-200.

42 J. H. Dai, Y. Song, B. Shi and R. Yang, *J. Phys. Chem. C*, 2013, **117**, 25374-25380.

43 B. Shi and Y. Song, *Int. J. Hydrogen Energy*, 2013, **38**, 6417-6424.

44 J. H. Dai, Y. Song and R. Yang, *Int. J. Hydrogen Energy*, 2011, **36**, 12939-12949.

45 A. J. Du, S. C. Smith and G. Q. Lu, *J. Phys. Chem. C*, 2007, **111**, 8360-8365.

46 J. Zhang, Y. N. Huang, C. Mao and P. Peng, *J. Alloy Compd.*, 2012, **538**, 205-211.

47 R. F. W. Bader, Chem. Rev., 1991, **91**, 893-928.

48 G. Henkelman, A. Arnaldsson and H. Jónsson, Comput. Mater. Sci., 2006, **36**, 354-360.

49 E. Sanville, S. D. Kenny, R. Smith and G. Henkelman, J. Comput. Chem. 2007, **28**, 899−908.